PHYSICAL REVIEW B **92**, 241115(R) (2015)

Proposed platform to study interaction-enabled topological phases with fermionic particles

Ching-Kai Chiu, D. I. Pikulin, and M. Franz
Department of Physics and Astronomy, University of British Columbia, Vancouver, British Columbia, Canada V6T 1Z1 and Quantum Matter Institute, University of British Columbia, Vancouver, British Columbia, Canada V6T 1Z4

(Received 11 February 2015; published 23 December 2015)

We propose a platform for interacting topological phases of fermions with time reversal symmetry $\bar{\Theta}$ (such that $\bar{\Theta}^2 = 1$) that can be realized in vortex lattices in the surface state of a topological insulator. The constituent particles are Majorana fermions bound to vortices and antivortices of such a lattice. We explain how the $\bar{\Theta}$ symmetry arises and discuss ways in which interactions can be experimentally tuned and detected. We show how these features can be exploited to realize a class of interaction-enabled crystalline topological phases that have no analog in weakly interacting systems.

DOI: 10.1103/PhysRevB.92.241115 PACS number(s): 74.20.−z, 71.10.Pm, 73.63.Nm, 75.75.−c

A theoretical understanding of the topological phases of noninteracting fermions, now thought to be complete, gave us a treasure trove of new materials over the past decade, including the topological insulators (both two and three dimensions) [1–4] and engineered topological superconductors with Majorana zero modes [5–8]. The same theoretical framework also opened new areas of inquiry, leading to concepts such as the Weyl semimetals, axion insulators, and topological exciton condensates that are actively pursued in experiments. When strong interactions are included, the situation becomes more complicated and the classification of topological phases less well understood, especially for fermionic systems [9]. It is expected that interacting systems could produce novel phases with unusual properties, such as excitations with fractionalized quantum numbers and unusual exchange statistics. Although a number of specific interaction-enabled topological phases with fermions have been theoretically proposed [10–18], the only such phases that are known to exist in the real world are the fractional quantum Hall states [19,20].

With the goal of enlarging the space of experimentally accessible topological phases that depend for their existence on strong interactions, we propose here a physical platform that realizes the paradigm of fermions with time reversal (TR) symmetry $\bar{\Theta}$ such that $\bar{\Theta}^2 = 1$. Interacting fermions with this property have been employed in seminal works by Fidkowski and Kitaev (FK) [21], who showed how the integer classification of their one-dimensional (1D) topological phases in the noninteracting limit changes to Z_8 classification when interactions are included. More recently, Lapa, Teo, and Hughes (LTH) [22] introduced a model with $\bar{\Theta}$ and an additional inversion symmetry $\mathcal{P}$. In this case, it turns out that there are no topologically nontrivial 1D phases in the absence of interactions. Remarkably, when interactions are included, a topologically nontrivial phase becomes possible (the interacting classification here is Z_2). The latter, then, is a genuine interaction-enabled topological phase that fundamentally cannot exist in the noninteracting limit.

The TR symmetry that we have in mind acts on the spinless fermion annihilation operator c_j through an operator $\bar{\Theta}$ so that $\bar{\Theta} c_j \bar{\Theta}^{-1} = c_j$ and $\bar{\Theta} i \bar{\Theta}^{-1} = -i$. If we decompose our Dirac fermion into a pair of Majorana fermions $c_j = \frac{1}{2}(\alpha_j + i\beta_j)$, it follows that

$$\bar{\Theta}\alpha_j\bar{\Theta}^{-1} = \alpha_j, \quad \bar{\Theta}\beta_j\bar{\Theta}^{-1} = -\beta_j. \tag{1}$$

In a $\bar{\Theta}$-invariant Hamiltonian expressed in terms of α_j,β_j operators only certain terms are allowed. For instance, bilinears $i\alpha_j\beta_k$ are allowed while $i\alpha_j\alpha_k$ and $i\beta_j\beta_k$ are prohibited. Similarly, four-fermion interaction terms with even numbers of α_j's are allowed, such as $\alpha_j\alpha_k\alpha_l\alpha_m$ or $\beta_j\beta_k\alpha_l\alpha_m$, but those with an odd number are not. Finding a physical system whose Hamiltonian implements the above symmetry constraints presents a challenge because electrons, the only relevant fermions in solids, have spin $\frac{1}{2}$ and the natural TR operation Θ for such spinful fermions satisfies $\Theta^2 = -1$. The important ideas [21–23] that involve fermions with $\bar{\Theta}$ such that $\bar{\Theta}^2 = 1$ have therefore remained largely untested (see, however, the proposal in Ref. [24]). In what follows, we show how the ingredients necessary to realize the phases envisioned by FK and LTH can be realized in a concrete physical system accessible with the available experimental methods.

A system we explore in this Rapid Communication is similar to that studied in Ref. [25]—a superconducting (SC) surface of a strong topological insulator (STI)—with one extra ingredient. In addition to vortices, which are known to harbor unpaired Majorana zero modes (MZMs) [26], we include in our considerations antivortices which also contain MZMs but, as we show, of a different type. Specifically, we demonstrate that it is consistent to assign the two types of Majorana fermions α_j,β_j that obey Eq. (1) to vortices and antivortices, respectively. Structures composed of vortices and antivortices, arranged such that their corresponding Majorana wave functions have nonzero overlaps, then implement $\bar{\Theta}$-invariant fermionic Hamiltonians with $\bar{\Theta}^2 = 1$. We discuss various vortex/antivortex geometries that realize interacting lattice models, including the LTH model [22] mentioned above.

We now proceed to substantiate these ideas and claims. The physical system, an STI with a superconducting surface, is described by the Fu-Kane Hamiltonian [26] $\mathcal{H} = \int d^2r\, \hat{\Psi}_{\boldsymbol{r}}^\dagger H_{\rm FK}(\boldsymbol{r})\hat{\Psi}_{\boldsymbol{r}}$, where $\hat{\Psi}_{\boldsymbol{r}} = (c_{\uparrow\boldsymbol{r}}, c_{\downarrow\boldsymbol{r}}, c_{\downarrow\boldsymbol{r}}^\dagger, -c_{\uparrow\boldsymbol{r}}^\dagger)^T$ is the Nambu spinor and

$$H_{\rm FK} = \tau^z(\boldsymbol{p}\cdot\boldsymbol{\sigma} - \mu) + \tau^x\Delta_1 + \tau^y\Delta_2. \tag{2}$$

Here, $\boldsymbol{\sigma},\boldsymbol{\tau}$ are Pauli matrices in spin and Nambu spaces, respectively, and $\Delta = \Delta_1 + i\Delta_2$ represents the SC order parameter. A single isolated vortex, expressed as $\Delta(\boldsymbol{r}) = \Delta_0(r)e^{-in\varphi}$ with φ the polar angle and $n = \pm 1$ corresponding to vortex or antivortex, respectively, is known to bind a MZM [26]. The Hamiltonian (2) respects the particle-hole symmetry $\mathcal{C}$ generated by $\Xi = \sigma^y \tau^y K$ ($\Xi^2 = +1, K$ denotes a complex conjugation) and, for a purely real gap function Δ, also the physical TR symmetry Θ generated by $\Theta = i\sigma^y K$ ($\Theta^2 = -1$). In the presence of vortices Θ is broken, but in the special case when $\mu = 0$, the Hamiltonian respects a fictitious TR symmetry $\bar{\Theta}$ with $\bar{\Theta} = \sigma^x \tau^x K$ ($\bar{\Theta}^2 = +1$), even in the presence of vortices [27]. From now on we focus on this $\mu = 0$ "neutrality point" with an extra symmetry. Together, the two symmetries Ξ and $\bar{\Theta}$ define a BDI class with chiral symmetry $\Pi = \Xi\bar{\Theta} = -\sigma^z \tau^z$.

Eigenstates of the Hamiltonian (2) are four-component Nambu spinors $\Phi(\boldsymbol{r}) = (u_\uparrow, u_\downarrow, v_\uparrow, v_\downarrow)^T$. Because the particle-hole symmetry $\mathcal{C}$ maps positive energy eigenstates to their negative energy partners, a nondegenerate zero mode $H_{\text{FK}}\Phi_0 = 0$ is self-conjugate under $\mathcal{C}$, that is, it obeys $\Xi\Phi_0 = \Phi_0$. This constrains its components such that $v_\uparrow = u_\downarrow^*$ and $v_\downarrow = -u_\uparrow^*$. In addition, because $\{H_{\text{FK}}, \Pi\} = 0$, the zero mode Φ_0 must be an eigenstate of Π. There are two choices that satisfy these conditions,

$$\Phi_0^{(+)} = (0, u_\downarrow, u_\downarrow^*, 0)^T, \quad \Phi_0^{(-)} = (u_\uparrow, 0, 0, -u_\uparrow^*)^T, \tag{3}$$

corresponding to the two eigenvalues $\nu = \pm 1$ of Π. It is easy to check that

$$\bar{\Theta}\Phi_0^{(\pm)} = \pm\Phi_0^{(\pm)}, \tag{4}$$

i.e., the two MZMs transform as even and odd under $\bar{\Theta}$. To complete the argument, we construct the corresponding zero-mode operators $\gamma_\pm = \int d^2r \Phi_0^{(\pm)}(\boldsymbol{r})^\dagger \hat{\Psi}_{\boldsymbol{r}}$. From Eqs. (3) and (4) it follows that

$$\gamma_\pm^\dagger = \gamma_\pm, \quad \bar{\Theta}\gamma_\pm\bar{\Theta}^{-1} = \pm\gamma_\pm. \tag{5}$$

The zero-mode operators are Majorana and the two types transform in the opposite way under $\bar{\Theta}$. Now, suppose that γ_+ with a wave function $\Phi_0^{(+)}$ resides in the core of a positive $n = 1$ vortex (as can be verified by an explicit calculation [25]). The physical TR symmetry Θ maps a vortex onto an antivortex because the direction of superflow is reversed under Θ. At the same time the corresponding operator Θ maps $\Phi_0^{(+)}$ to $\Phi_0^{(-)}$. Antivortex thus necessarily carries the other type of Majorana represented by γ_-. Comparing Eqs. (5) and (1), we conclude that vortices and antivortices in the Fu-Kane model at neutrality carry MZMs that transform as even and odd, respectively, under $\bar{\Theta}$ and can thus be assigned as α_j, β_j Majorana operators in models with $\bar{\Theta}^2 = 1$. We note that these results can be explicitly checked by a direct calculation of the zero-mode wave functions [8] in Hamiltonian (2).

Systems in this symmetry class composed of only vortices and no antivortices admit interaction terms of the form $g\alpha_j\alpha_k\alpha_l\alpha_m$ but no bilinear terms and are thus inherently strongly interacting. Some models of this type have been explored in Ref. [25]. When the system is slightly detuned from neutrality, then $\bar{\Theta}$ is broken and bilinears $it'\alpha_j\alpha_k$ become allowed with $t' \sim \mu$. In the following, we shall adopt an assumption that μ has been tuned sufficiently close to zero so that $t' \ll g$ and we may thus neglect all bilinears prohibited by $\bar{\Theta}$.

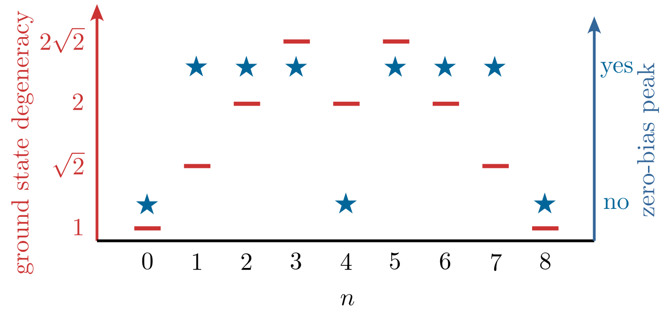

FIG. 1. (Color online) Ground state degeneracy in a cluster with n vortices and generic interaction terms. Stars denote the presence or absence of zero bias peaks in vortices observable by STM.

As our first example of interesting structures that can be constructed with these ingredients, we consider a cluster made with a small number n of vortices. As we shall argue, scanning tunneling microscopy (STM) can be used to probe the effects of interactions in such a small cluster by examining the vortex core spectra for the presence or absence of MZMs. We envision changing the total vorticity n of our cluster from 0 to 8 by adding vortices one by one to observe the theoretically predicted Z_8 periodicity [21,23] generated in the presence of interactions. In the absence of interactions the ground state has degeneracy $2^{n/2}$ and STM will observe a single MZM in each vortex. When interactions are present, STM should still see zero modes for $n = 1,2,3$ and for all odd values of n, but the zero modes could generically split for even $n \geqslant 4$, because an interaction term can be first constructed with four Majorana operators. The pattern of ground state degeneracies we obtain for a system of n vortices with generic interactions allowed by $\bar{\Theta}$ is displayed in Fig. 1 and is consistent with results of Ref. [23]. We find that MZMs, detectable by STM, will be present for all n except when $n = 4k$ with k integer. This is to be contrasted with a noninteracting case with generic hopping terms allowed (e.g., when $\mu \neq 0$); here, the ground state degeneracy is $\sqrt{2}(n \bmod 2)$ and zero bias peaks will be seen for all odd n.

As an example of considerations that lead to Fig. 1, we now discuss the special cases of an interacting system with $n = 4k$. We start with $n = 4$, denote the Majorana operators as $\alpha_1, \alpha_1', \alpha_2, \alpha_2'$, and define complex fermions $d_l = \frac{1}{2}(\alpha_l + i\alpha_l')$. Noting that $i\alpha_l\alpha_l' = 2n_l - 1$ where $n_l = d_l^\dagger d_l$ is the number operator, we may label the quantum states of the four Majorana fermions in the cluster by the eigenvalues $n_l = 0,1$ as $|n_1 n_2\rangle$. The most general interaction term $h_4 = g\alpha_1\alpha_2\alpha_1'\alpha_2'$ splits the fourfold degeneracy into an even parity ground state doublet $|00\rangle, |11\rangle$ (for $g > 0$) and odd parity excited states $|01\rangle, |10\rangle$. Because both ground states have the same parity, single-electron tunneling will necessarily cause transitions to the excited states and the STM peaks will appear at energies $\pm 2g$, not zero.

For $n = 8$ we consider a specific pattern displayed in Fig. 2(a). This pattern is easy to analyze and also forms the basic building block for the interaction-enabled LTH topological crystalline phase that we shall discuss below. As argued previously [25], the strongest interactions occur for those groups of four Majorana fermions that are spaced most

RAPID COMMUNICATIONS

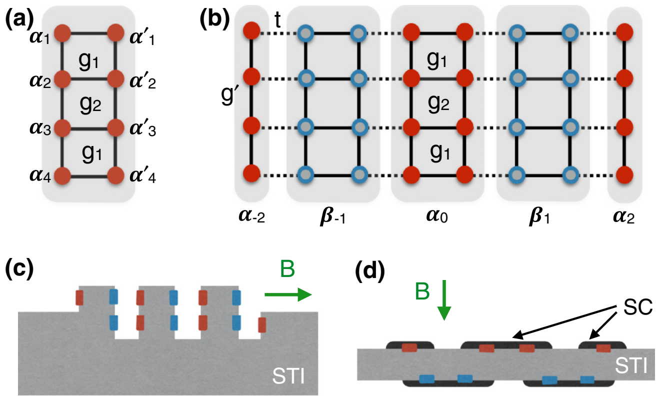

FIG. 2. (Color online) Vortex lattice geometries for interacting Majorana models. Solid (open) circles represent vortices (antivortices), while solid and dashed lines indicate hopping and interaction terms, respectively, consistent with $\bar{\Theta}$. (a) Cluster of eight vortices. (b) The four-leg LTH ladder invariant under both $\bar{\Theta}$ and $\mathcal{P}$. Possible experimental realizations are sketched in (c) and (d). In (c) the STI surface is assumed to be superconducting and the thickness of the STI sufficiently large so that the Majorana wave-function overlaps occur predominantly in the surface. Under these conditions the setup will realize the LTH ladder depicted in (b). In (d) the interactions take place in the surfaces but tunneling is assumed to occur through the bulk of the flake.

closely together. This is because the corresponding coupling constants depend on the overlap of the exponentially decaying Majorana wave functions. With this in mind, we identify the dominant interaction terms associated with the square plaquettes in Fig. 2(a) described by

$$h_\square = g_1(\alpha_1\alpha_1'\alpha_2\alpha_2' + \alpha_3\alpha_3'\alpha_4\alpha_4') + g_2\alpha_2\alpha_2'\alpha_3\alpha_3'. \qquad (6)$$

For $g_1,g_2 > 0$ the ground state of $h_\square$ is doubly degenerate, spanned by eigenvectors $|0000\rangle$ and $|1111\rangle$ in the same notation as above. The energy is $E_g = -2g_1 - g_2$. The subdominant interaction term is associated with two straight legs,

$$h_| = g'(\alpha_1\alpha_2\alpha_3\alpha_4 + \alpha_1'\alpha_2'\alpha_3'\alpha_4'). \qquad (7)$$

It is easy to see that the inclusion of $h_|$ splits the ground state doublet of $h_\square$ into a bonding/antibonding pair with $|\psi_\pm\rangle = (|0000\rangle \pm |1111\rangle)/\sqrt{2}$. For $g' > 0$ the unique ground state of

$$h_8 = h_\square + h_| \qquad (8)$$

is $|\psi_-\rangle$, while $|\psi_+\rangle$ is the first excited state with energy $4g'$.

Now consider the four-leg chain depicted in Fig. 2(b). This is a version of the LTH model [22] that can be constructed using our platform. It consists of alternating clusters of eight vortices and antivortices, each described by the interacting Hamiltonian $h_8(\boldsymbol{\alpha}_{2j})$ and $h_8(\boldsymbol{\beta}_{2j+1})$, connected by nearest-neighbor hopping terms with amplitude t. Here, $\boldsymbol{\alpha}_{2j}$ denotes the octet of $\{\alpha_l,\alpha_l'\}$ operators in cluster $2j$ and the same for $\boldsymbol{\beta}_{2j+1}$. The Hamiltonian then reads

$$H_{\mathrm{LTH}} = \sum_{j=-N}^{N} h_8(\boldsymbol{\alpha}_{2j}) + \sum_{j=-N-1}^{N} h_8(\boldsymbol{\beta}_{2j+1}) + h_|^{\mathrm{edge}}$$
$$-it\sum_{j=-N-1}^{N+1}(\alpha_{l,2j}'\beta_{l,2j+1} + \beta_{l,2j-1}'\alpha_{l,2j}), \qquad (9)$$

where $h_|^{\mathrm{edge}}$ has a form indicated in Eq. (7) and describes the four dangling Majoranas at the two ends of the chain. The Hamiltonian (9) respects $\bar{\Theta}$ as well as the inversion symmetry $\mathcal{P}$. The latter is generated by $\{\alpha_{l,j},\alpha_{l,j}'\} \to \{\alpha_{l,-j}',\alpha_{l,-j}\}$ and $\{\beta_{l,j},\beta_{l,j}'\} \to -\{\beta_{l,-j}',\beta_{l,-j}\}$.

Without interactions, there exist no topologically nontrivial phases in a system with these symmetries [22]. Indeed, we see that when $g_1 = g_2 = g' = 0$ and $t \neq 0$, the system breaks up into a set of local dimers formed by $\alpha\beta$ products on the dashed bonds in Fig. 2(b). The ground state is unique with a gap $2t$ to the lowest excitation and clearly topologically trivial.

In the opposite limit, $t = 0$ and $g_1 \simeq g_2 > g' > 0$, the ground state is a direct product of $|\psi_-\rangle_j$ states on each cluster j. If we impose periodic boundary conditions, the ground state is unique with a gap $4g'$ to the lowest excited state. However, for an open chain that preserves the symmetries, as the one indicated in Fig. 2(b), there is a *fourfold degeneracy* associated with $h_|^{\mathrm{edge}}$. The four independent quantum states associated with the quartet of α_l Majoranas at each end are split by $h_|^{\mathrm{edge}}$ into a doubly degenerate ground state (with even local parity) and a doubly degenerate excited state (with odd parity). As noted in Ref. [22], $\bar{\Theta}$ connects the two degenerate ground states, but its action in this subspace is *anomalous* with $\bar{\Theta}^2 = -1$. The edge modes therefore comprise two effective spin-$\frac{1}{2}$ degrees of freedom and constitute fractionalized excitations analogous to those appearing in spin-1 Haldane chains [28,29]. In a long chain the edge degeneracy is therefore protected by the Kramers theorem and cannot be removed by any local perturbation preserving $\bar{\Theta}$. It signals a topological phase, one that fundamentally cannot exist in a noninteracting system. If we turn on a small hopping t, the topological phase should persist up to a critical strength t_c of order g', at which point a phase transition occurs to the trivial phase.

We have confirmed the above picture by performing exact numerical diagonalizations of H_{LTH}; the results are displayed in Fig. 3. Our simulations with periodic boundary conditions [Fig. 3(a)] indicate a phase transition marked by the excitation gap closing at $g_c \simeq 0.81t$, obtained by extrapolating the energy minimum to $L_x \to \infty$. Figure 3(b) confirms that with open boundary conditions the ground state is unique for $g < g_c$ but becomes fourfold degenerate for $g > g_c$ with all ground states in the same parity sector, in accord with our expectation for the interaction-enabled topological phase.

As explained in the Supplemental Material [30], a system described by the LTH Hamiltonian (9) can be regarded as a "$4e$ superconductor." (This is because it breaks the fermion number conservation symmetry while all the anomalous expectation values that are bilinear, such as $\langle d_1d_2\rangle$, vanish.) The authors of Ref. [22] proposed to look for physical realizations of such a $4e$ superconductor in certain pair density wave systems, discussed theoretically in the context of underdoped high-T_c cuprate

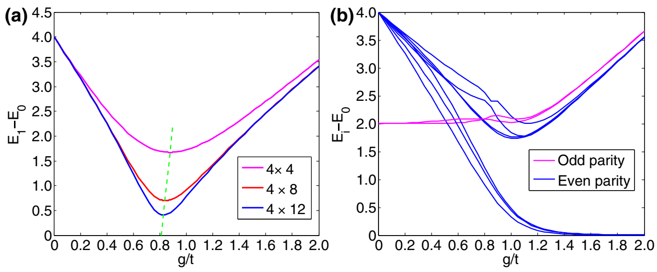

FIG. 3. (Color online) Excitation energies of the LTH Hamiltonian (9) obtained by exact numerical diagonalization. (a) The lowest excitation energy in a system of length $L_x = 4,8,12$ with periodic boundary conditions. (b) Several lowest excitation energies for $L_x = 8$ and open boundary conditions. We take $g_1 = g_2 = g' \equiv g$ and the energies are in the units of t.

superconductors [31]. Whether or not such a phase exists in real materials remains to be seen. Our proposed realization of the LTH model, on the other hand, relies on ingredients that are known to exist. Specifically, SC order in the surface state of an STI has been experimentally observed by a number of groups [32–42]. In some cases the chemical potential has been tuned to the close vicinity of the Dirac point [39,40], as required for models with symmetry $\bar{\Theta}$. Vortex cores [42], and the expected MZMs, have also been imaged [43]. Assembling vortices into regular structures, controlling their geometry, and reliably probing the zero modes remains a challenge, but it is one that does not seem insurmountable given the recent progress.

In the near term it should be possible to probe the effects of interactions in small clusters of vortices by STM, as we discussed. The relevant energy scale can be quite large, ∼10 meV, under favorable conditions [25] and should permit observation of the interaction-induced Z_8 periodicity. To engineer the LTH model, the key challenge will be to assemble stable arrays containing both vortices and antivortices in close proximity to one another. We note that such structures have been observed to occur spontaneously in mesoscopic SC samples with certain geometries [44]. Alternately, one can leverage the fact that in a thin STI/SC film or flake a uniform perpendicular field B will produce vortices on the top surface and antivortices on the bottom surface. Figures 2(c) and 2(d) outline two possible experimental realizations of the LTH vortex/antivortex lattice exploiting this principle [45].

The interaction-enabled topological phases discussed in this work are gapped and therefore robust with respect to moderate amounts of symmetry-preserving disorder. Specifically, disorder in vortex positions does not break $\bar{\Theta}$ and is therefore innocuous. It also follows that fine details of the geometry sketched in Figs. 2(a) and 2(b) are unimportant as long as $\bar{\Theta}$ and $\mathcal{P}$ are preserved to a good approximation. Any experimental realization that reasonably approximates the proposed model geometry should show the topological phase. Local fluctuations in the chemical potential break $\bar{\Theta}$, but we expect the gapped phases to remain robust as long as the symmetry is preserved on average and the fluctuations do not exceed the gap amplitude [30,46].

The authors are indebted to NSERC, CIfAR, and Max Planck–UBC Centre for Quantum Materials for support. M.F. acknowledges The Aspen Center for Physics and IQMI at Caltech for hospitality during the initial stages of this project.

[1] M. Z. Hasan and C. L. Kane, Rev. Mod. Phys. **82**, 3045 (2010).
[2] J. E. Moore, Nature (London) **464**, 194 (2010).
[3] X.-L. Qi and S.-C. Zhang, Rev. Mod. Phys. **83**, 1057 (2011).
[4] M. Franz and L. Molenkamp, *Topological Insulators* (Elsevier, New York, 2013).
[5] J. Alicea, Rep. Prog. Phys. **75**, 076501 (2012).
[6] C. W. J. Beenakker, Annu. Rev. Condens. Matter Phys. **4**, 113 (2013).
[7] T. D. Stanescu and S. Tewari, J. Phys.: Condens. Matter **25**, 233201 (2013).
[8] S. R. Elliott and M. Franz, Rev. Mod. Phys. **87**, 137 (2015).
[9] X.-G. Wen, Phys. Rev. B **89**, 035147 (2014), and references therein.
[10] D. J. Clarke, J. Alicea, and K. Shtengel, Nat. Commun. **4**, 1348 (2013).
[11] N. H. Lindner, E. Berg, G. Refael, and A. Stern, Phys. Rev. X **2**, 041002 (2012).
[12] A. Vaezi, Phys. Rev. B **87**, 035132 (2013).
[13] M. Barkeshli and X.-L. Qi, Phys. Rev. X **2**, 031013 (2012).
[14] C. Wang, A. C. Potter, and T. Senthil, Phys. Rev. B **88**, 115137 (2013).
[15] M. A. Metlitski, C. L. Kane, and M. P. A. Fisher, Phys. Rev. B **92**, 125111 (2015)
[16] P. Bonderson, C. Nayak, and X.-L. Qi, J. Stat. Mech. (2013) P09016.
[17] X. Chen, L. Fidkowski, and A. Vishwanath, Phys. Rev. B **89**, 165132 (2014).
[18] R. S. K. Mong, D. J. Clarke, J. Alicea, N. H. Lindner, P. Fendley, C. Nayak, Y. Oreg, A. Stern, E. Berg, K. Shtengel, and M. P. A. Fisher, Phys. Rev. X **4**, 011036 (2014).
[19] D. C. Tsui, H. L. Stormer, and A. C. Gossard, Phys. Rev. Lett. **48**, 1559 (1982).
[20] R. B. Laughlin, Phys. Rev. Lett. **50**, 1395 (1983).
[21] L. Fidkowski and A. Kitaev, Phys. Rev. B **81**, 134509 (2010); **83**, 075103 (2011).
[22] M. F. Lapa, J. C. Y. Teo, and T. L. Hughes, arXiv:1409.1234.
[23] A. M. Turner, F. Pollmann, and E. Berg, Phys. Rev. B **83**, 075102 (2011).
[24] C. Fang, M. J. Gilbert, and B. A. Bernevig, Phys. Rev. Lett. **112**, 106401 (2014).
[25] C.-K. Chiu, D. I. Pikulin, and M. Franz, Phys. Rev. B **91**, 165402 (2015).
[26] L. Fu and C. L. Kane, Phys. Rev. Lett. **100**, 096407 (2008).
[27] J. C. Y. Teo and C. L. Kane, Phys. Rev. B **82**, 115120 (2010).
[28] F. D. M. Haldane, Phys. Lett. A **93**, 464 (1983).
[29] I. Affleck, T. Kennedy, E. H. Lieb, and H. Tasaki, Phys. Rev. Lett. **59**, 799 (1987).
[30] See Supplemental Material at http://link.aps.org/supplemental/10.1103/PhysRevB.92.241115 for additional information and discussion of the effect of potential disorder, further comments

on the realization of the LTH model and its connections with the 4e superconductor.

[31] E. Berg, E. Fradkin, and S. A. Kivelson, Nat. Phys. **5**, 830 (2009).
[32] G. Koren, T. Kirzhner, E. Lahoud, K. B. Chashka, and A. Kanigel, Phys. Rev. B **84**, 224521 (2011).
[33] B. Sacépé, J. B. Oostinga, J. Li, A. Ubaldini, N. J. G. Couto, E. Giannini, and A. F. Morpurgo, Nat. Commun. **2**, 575 (2011).
[34] M.-X. Wang, C. Liu, J.-P. Xu, F. Yang, L. Miao, M.-Y. Yao, C. L. Gao, C. Shen, X. Ma, X. Chen, Z.-A. Xu, Y. Liu, S.-C. Zhang, D. Qian, J.-F. Jia, and Q.-K. Xue, Science **336**, 52 (2012).
[35] F. Qu, F. Yang, J. Shen, Y. Ding, J. Chen, Z. Ji, G. Liu, J. Fan, X. Jing, C. Yang, and L. Lu, Sci. Rep. **2**, 339 (2012).
[36] J. R. Williams, A. J. Bestwick, P. Gallagher, S. S. Hong, Y. Cui, A. S. Bleich, J. G. Analytis, I. R. Fisher, and D. Goldhaber-Gordon, Phys. Rev. Lett. **109**, 056803 (2012).
[37] E. Wang, H. Ding, A. V. Fedorov, W. Yao, Z. Li, Y.-F. Lv, K. Zhao, L.-G. Zhang, Z. Xu, J. Schneeloch, R. Zhong, S.-H. Ji, L. Wang, K. He, X. Ma, G. Gu, H. Yao, Q.-K. Xue, X. Chen, and S. Zhou, Nat. Phys. **9**, 621 (2013).
[38] Q. L. He, H. Liu, M. He, Y. H. Lai, H. He, G. Wang, K. T. Law, R. Lortz, J. Wang, and I. K. Sou, Nat. Commun. **5**, 4247 (2014).
[39] S. Cho, B. Dellabetta, A. Yang, J. Schneeloch, Z. Xu, T. Valla, G. Gu, M. J. Gilbert, and N. Mason, Nat. Commun. **4**, 1689 (2013).
[40] L. Zhao, H. Deng, I. Korzhovska, J. Secor, M. Begliarbekov, Z. Chen, E. Andrade, E. Rosenthal, A. Pasupathy, V. Oganesyan, and L. Krusin-Elbaum, arXiv:1408.1046.
[41] S.-Y. Xu, N. Alidoust, I. Belopolski, A. Richardella, C. Liu, M. Neupane, G. Bian, S.-H. Huang, R. Sankar, C. Fang, B. Dellabetta, W. Dai, Q. Li, M. J. Gilbert, F. Chou, N. Samarth, and M. Zahid Hasan, Nat. Phys. **10**, 943 (2014).
[42] J.-P. Xu, C. Liu, M.-X. Wang, J. Ge, Z.-L. Liu, X. Yang, Y. Chen, Y. Liu, Z.-A. Xu, C.-L. Gao, D. Qian, F.-C. Zhang, and J.-F. Jia, Phys. Rev. Lett. **112**, 217001 (2014).
[43] J.-P. Xu, M.-X. Wang, Z. L. Liu, J.-F. Ge, X. Yang, C. Liu, Z. A. Xu, D. Guan, C. L. Gao, D. Qian, Y. Liu, Q.-H. Wang, F.-C. Zhang, Q.-K. Xue, and J.-F. Jia, Phys. Rev. Lett. **114**, 017001 (2015).
[44] L. F. Chibotaru, A. Ceulemans, V. Bruyndoncx, and V. V. Moshchalkov, Nature (London) **408**, 833 (2000).
[45] D. I. Pikulin, C.-K. Chiu, X. Zhu, and M. Franz, Phys. Rev. B **92**, 075438 (2015).
[46] A. Milsted, L. Seabra, I. C. Fulga, C. W. J. Beenakker, and E. Cobanera, Phys. Rev. B **92**, 085139 (2015).